

Pore Water Pressure Behavior during Liquefaction Based on Shaking Table Testing

Muhammad Yunus^{1,*}, Achmad Bakri Muhiddin², Tri Harianto², Ardy Arsyad²

¹Doctoral Program in Department of Civil Engineering, Faculty of Engineering, Hasanuddin University, Indonesia

²Department of Civil Engineering, Faculty of Engineering, Hasanuddin University, Indonesia

Received October 27, 2025; Revised February 27, 2026; Accepted March 26, 2026

Cite This Paper in the Following Citation Styles

(a): [1] Muhammad Yunus, Achmad Bakri Muhiddin, Tri Harianto, Ardy Arsyad, "Pore Water Pressure Behavior during Liquefaction Based on Shaking Table Testing," *Civil Engineering and Architecture*, Vol. 14, No. 3, pp. 1543 - 1554, 2026. DOI: 10.13189/cea.2026.140312.

(b): Muhammad Yunus, Achmad Bakri Muhiddin, Tri Harianto, Ardy Arsyad (2026). Pore Water Pressure Behavior during Liquefaction Based on Shaking Table Testing. *Civil Engineering and Architecture*, 14(3), 1543 - 1554. DOI: 10.13189/cea.2026.140312.

Copyright©2026 by authors, all rights reserved. Authors agree that this article remains permanently open access under the terms of the Creative Commons Attribution License 4.0 International License

Abstract Liquefaction is a critical geotechnical hazard that occurs when excess pore water pressure builds up in saturated sandy soils during earthquakes, leading to a significant reduction in effective stress and shear strength. This study investigates the behavior of pore water pressure during liquefaction using shaking table tests on a laboratory-scale saturated sand model with an initial relative density of 40%. Sinusoidal horizontal excitations were applied with peak ground accelerations (PGA) of 0.3 g, 0.4 g, and 0.5 g for a duration of 60 seconds. Excess pore water pressure was continuously monitored using piezometer sensors installed at depths of 100 mm, 300 mm, and 500 mm to capture depth-dependent responses. The results reveal a nonlinear relationship between PGA and pore water pressure response. The highest excess pore water pressure (Δu) and pore water pressure ratio (ru) were recorded at PGA = 0.3 g, particularly at greater depths, indicating that moderate seismic loading promotes pore pressure accumulation under limited drainage conditions. At higher PGA levels (0.4 g and 0.5 g), pore water pressure did not increase proportionally, suggesting the influence of cyclic soil densification and accelerated dissipation mechanisms. Temporally, the pore water pressure response can be divided into three phases: rapid buildup, peak response approaching liquefaction, and subsequent dissipation. These findings demonstrate that liquefaction potential cannot be evaluated solely based on earthquake acceleration intensity, but must also consider soil depth, density, and drainage characteristics, providing useful insights for liquefaction risk assessment and mitigation.

Keywords Pore Water Pressure Ratio, Liquefaction, Shaking Table, Peak Ground Acceleration, Sandy Soil

1. Introduction

Indonesia, located within the Pacific Ring of Fire, is highly vulnerable to seismic activity. Several past earthquake events, such as the 2004 Aceh [1], 2009 Padang [2], 2018 Palu [3], and 2021 Majene [4] earthquakes, have demonstrated the severe consequences of soil liquefaction. Liquefaction occurs when water-saturated soil experiences an increase in pore water pressure. This reduces the soil's effective stress, resulting in a loss of shear strength and behavior resembling that of a fluid. This can have serious consequences for the stability of building foundations, embankments, port facilities, and flood barriers.

In this mechanism, the repeated vibrations caused by earthquakes compact the soil particles. Under limited drainage conditions, pore water cannot escape. This leads to an accumulation of pore water pressure (Δu), which reduces effective stress (σ'). When effective stress approaches zero, the soil loses its shear strength and liquefies [5], [6]. Therefore, it is very important to understand the effect of pore water pressure on liquefaction potential, especially in subsoil that supports strategic infrastructure [7].

In order to design appropriate mitigation strategies, it is

crucial to understand how saturated soil responds dynamically to seismic loads. However, direct observation in the field is significantly limited by the uncertainty of soil conditions, variations in earthquake intensity, and the difficulty of monitoring pore water pressure and deformation in real time [5], [6]. Therefore, shaking table-based laboratory testing is an effective alternative for simulating controlled earthquake loads and analyzing the dynamic behavior of soil and structures [8], [9].

Shaking table testing allows researchers to analyze the formation of excess pore water pressure [10], deformation [11], energy dissipation [12], and seismic wave propagation in laboratory-scale soil models. This simulation allows liquefaction characteristics and the dynamic response of soil to be identified in a more measurable and in-depth manner. Additionally, this method is crucial for evaluating the effectiveness of various soil reinforcement systems, including timber piles, hybrid piles, stone columns, and densification techniques, in mitigating liquefaction and deformation risks associated with seismic loads.

Although many previous studies have examined liquefaction through shaking table testing, most are limited to variations in input acceleration [13] or specific types of sand [14]. Few have comprehensively examined the effects of dynamic pore water pressure, damping, and deformation on reinforced and unreinforced models. Furthermore, few studies have combined simultaneous measurements of pore water pressure, soil acceleration, and surface subsidence in order to gain a more complete mechanistic understanding of how saturated soil responds to earthquake vibration cycles.

This study investigates pore water pressure behavior in

saturated sandy soil during liquefaction under varying PGA (0.3 g, 0.4 g, and 0.5 g) using shaking table tests on a laboratory-scale model with an initial relative density of 40%. The results provide insight into liquefaction mechanisms and the influence of earthquake acceleration on liquefaction potential, with implications for liquefaction risk mitigation.

2. Materials and Methods

2.1. Material Properties

The sand used in this study was collected from the coastal area of Galesong, Takalar Regency, South Sulawesi Province, Indonesia. The geographical location of the sampling site is shown in Figure 1, while representative sand samples are presented in Figure 2. The sand is classified as iron sand, characterized by a high heavy mineral content dominated by magnetite, with a specific gravity greater than 2.70.

Laboratory testing of the sand properties was conducted in accordance with ASTM 4254-16 [15] and ASTM 4253-16 [16] to determine the minimum and maximum dry unit weights and relative density parameters. The index properties of the Galesong sand are summarized in Table 1, while the corresponding grain size distribution curve is shown in Figure 3. Grain size distribution analysis indicates that the sand is uniformly graded, with a coefficient of uniformity ($C_u = 2.21$) and coefficient of curvature ($C_c = 1.02$). Based on its gradation characteristics, the sand falls within the range of soils susceptible to liquefaction.



Figure 1. Location of Galesong in Takalar Regency, South Sulawesi Province, Indonesia



Figure 2. Galesong sand

Table 1. Index Properties of Galesong Sand

No	Description	Unit	Value
1.	Water content (w)	%	18.26
2.	Specific gravity (G_s)	-	3.17
3.	Grain size distribution		
	a. D_{10}	mm	0.120
	b. D_{30}	mm	0.180
	c. D_{60}	mm	0.265
	d. Coefficient of uniformity (C_u)	-	2.21
	e. Coefficient of curvature (C_c)	-	1.02
4.	Unit weight (γ_d)		
	a. (γ_{dmin})	kN/m ³	18.25
	b. (γ_{dmax})	kN/m ³	20.21
5.	Void ratio (e)		
	a. (e_{min})	-	0.65
	b. (e_{max})	-	0.86

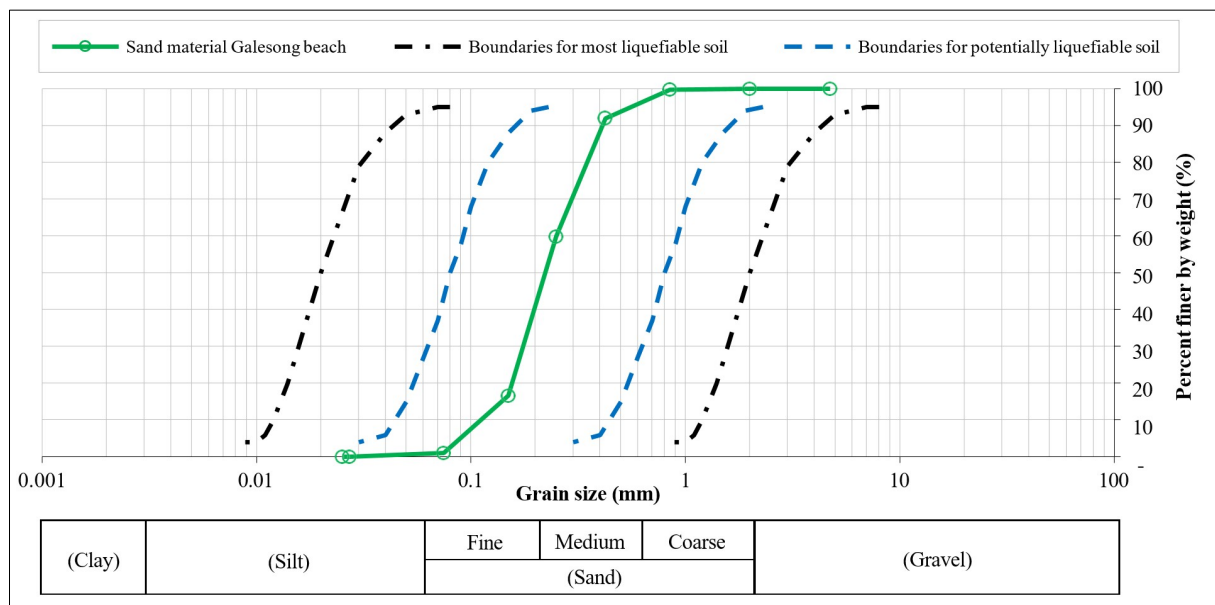


Figure 3. Distribution of Galesong sand grain sizes

2.2. Experimental Setup

Shaking table tests were conducted at the Geotechnical and Geoenvironmental Laboratory, Faculty of Engineering, Hasanuddin University. The shaking table has dimensions of 1.2 m × 1.2 m and a load capacity of 3 tonnes. Horizontal excitation is generated using a servo-hydraulic actuator, with a maximum displacement of 40 mm, an operating frequency range of 0.01–50 Hz, and an acceleration capacity up to 1 g. The loading parameters were controlled digitally to ensure repeatable input motions.

A transparent test tank with internal dimensions of 1200 mm × 1000 mm × 800 mm (length × width × height) was used to allow visual observation of soil behavior during testing. The tank was constructed from 10mm-thick acrylic panels reinforced with a steel frame. To reduce wave reflection from rigid boundaries, polyurethane foam boards were installed along the inner walls of the tank, following recommendations from previous shaking table studies [17], [18], [19]. The experimental setup, including the shaking table and test tank configuration, is shown in Figures 4 and 5.

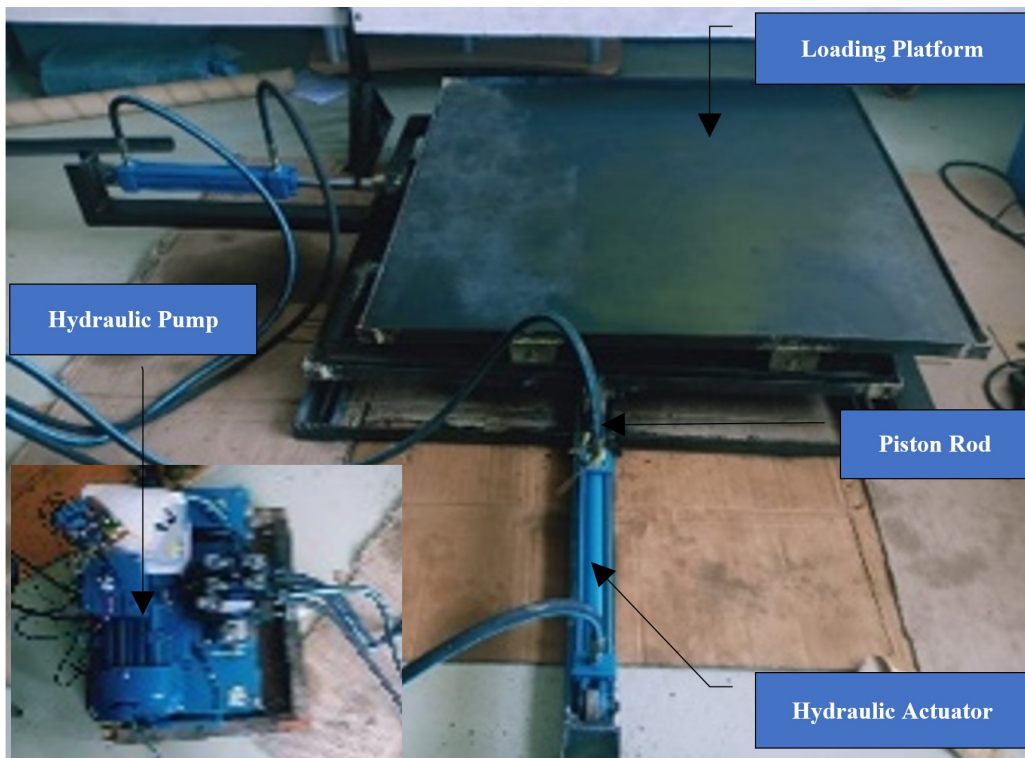


Figure 4. Shaking table

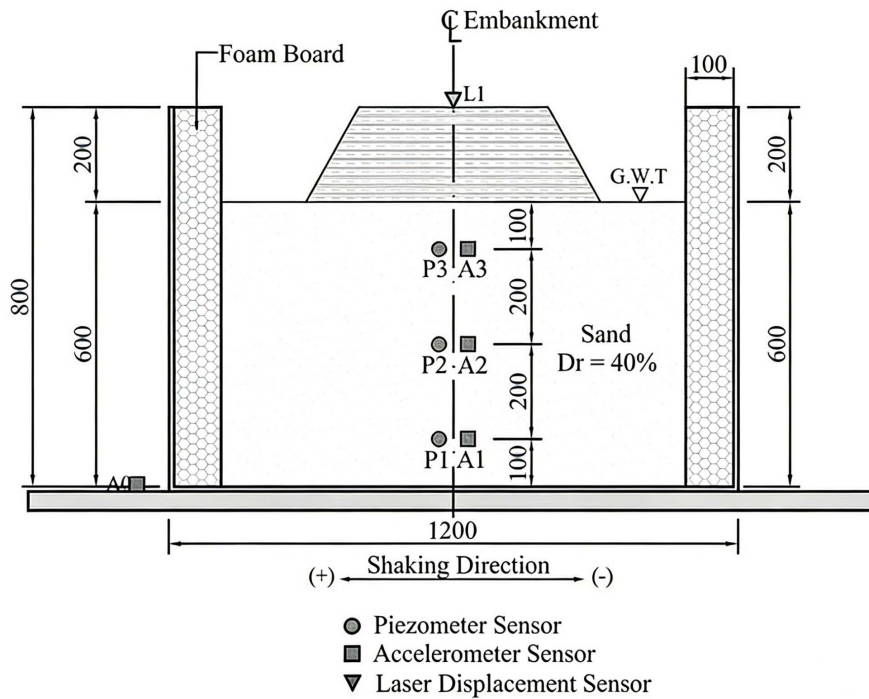


Figure 5. Test tank

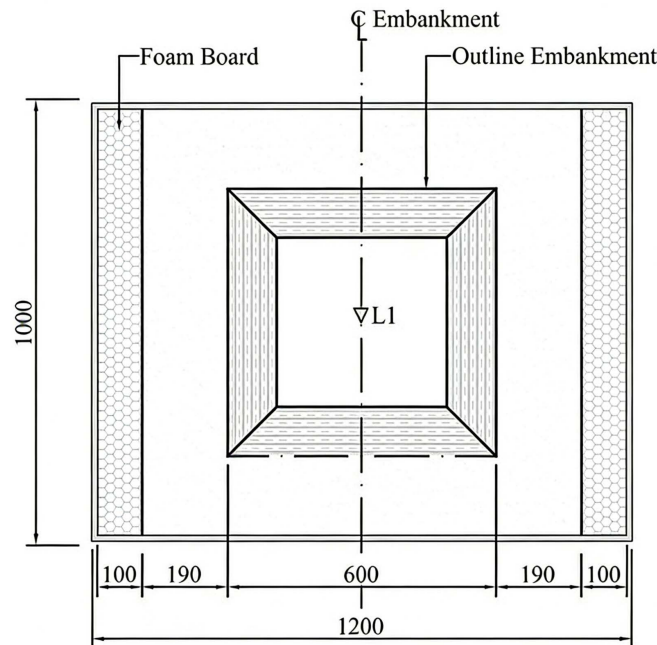
2.3. Physical Model Preparation and Instrumentation

The physical model was prepared using the sand bed saturation method. Dry sand was placed in six layers to achieve a total thickness of 600 mm with an initial relative density of 40%. Each layer was placed with a controlled drop height of 20 cm to maintain uniform density. The total dry weight of sand used in the model was 1,167.12 kg.

During sand placement, three piezometer sensors (P1, P2, and P3) were installed at depths of 50 cm, 30 cm, and 10 cm, respectively, to monitor excess pore water pressure development. In addition, three accelerometers (A1, A2, and A3) were installed to record soil acceleration at different elevations. The layout of the sensors and the overall physical model configuration are illustrated in Figure 6.



(a)



(b)

Figure 6. Layout of the experimental model, (a) Cross-sectional view of the model, (b) Top view of the model

After placement, the sand layer was saturated by slowly introducing water from the bottom of the tank until the water level exceeded the sand surface by approximately 1 cm. The saturated sand was then left undisturbed for 24 hours to ensure uniform pore water pressure distribution. An embankment model made of compacted clay with a slope angle of 60° was subsequently placed on top of the saturated sand layer to represent surface loading conditions.

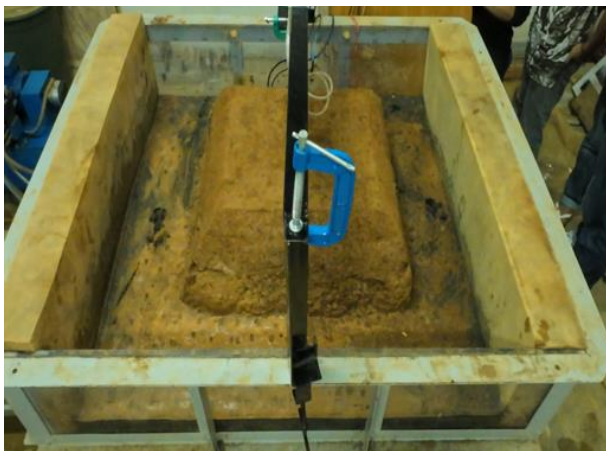
2.4. Loading Protocol and Test Procedure

The experimental program was designed to investigate the effect of peak ground acceleration (PGA) on pore water pressure behavior and liquefaction potential. Sinusoidal horizontal excitations with PGA values of 0.3 g, 0.4 g, and 0.5 g were applied to the model at a constant frequency for a duration of 60 seconds. These acceleration levels represent light to strong earthquake loading conditions.

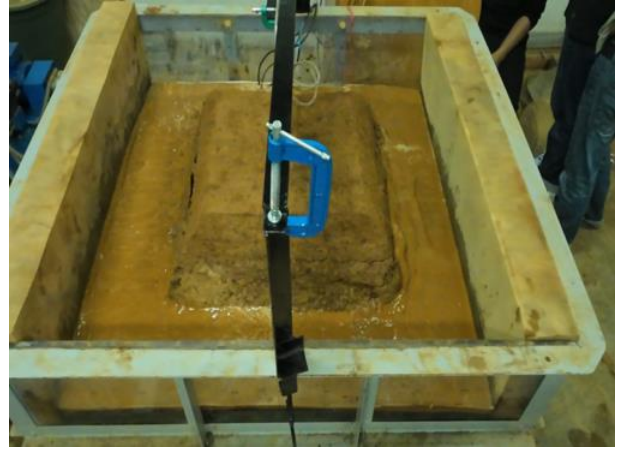
Each test was conducted under identical initial conditions to allow direct comparison of results. The testing matrix is presented in Table 2, and the physical condition of the model before and after testing is shown in Figure 7. Excess pore water pressure and acceleration responses were recorded continuously throughout the loading duration.

Table 2. Physical model testing matrix

Code	Dr (%)	PGA (g)	Time (second)
PGA 0.3 g	40	0.3	60
PGA 0.4 g	40	0.4	60
PGA 0.5 g	40	0.5	60



(a)



(b)

Figure 7. Physical model condition, (a) Before testing, (b) After testing

2.5. Pore Water Pressure Ratio

The pore water pressure ratio (ru) is used as an indicator to evaluate the liquefaction potential of saturated sand during shaking table testing. The parameter represents the ratio between the excess pore water pressure (Δu) and the initial effective vertical overburden stress (σ'_{v0}), and is defined as:

$$ru = \frac{\Delta u}{\sigma'_{v0}} \quad (1)$$

A value of $ru = 1$ indicates that the excess pore water pressure (Δu) is equal to the initial effective stress, resulting in a zero effective stress in the soil. This condition describes soil that has lost all its shear strength and is susceptible to liquefaction.

The initial effective vertical overburden stress (σ'_{v0}) corresponding to each piezometer depth (Table 3) was adopted in the calculation of the excess pore water pressure ratio (ru) using Equation (1), thereby providing a consistent reference stress for evaluating liquefaction potential.

Table 3. Initial effective overburden stress (σ'_{v0}) at different piezometer depths used in the calculation of the pore water pressure ratio (ru)

No.	Depth (mm)	γ (kN/m ³)	γ_w (kN/m ³)	σ_{v0} (kPa)	u (kPa)	σ'_{v0} (kPa)
1.	0	22.51	9.81	0.00	0.00	0.00
2.	100	22.51	9.81	2.25	0.98	1.27
3.	200	22.51	9.81	4.50	1.96	2.54
4.	300	22.51	9.81	6.75	2.94	3.81
5.	400	22.51	9.81	9.00	3.92	5.08
6.	500	22.51	9.81	11.25	4.91	6.35

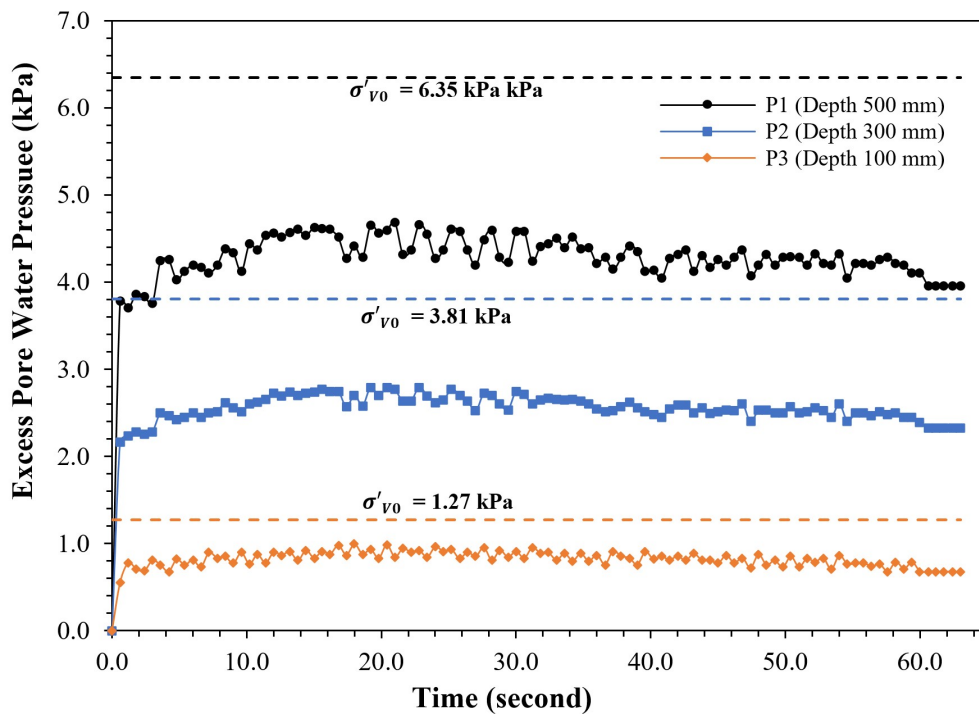
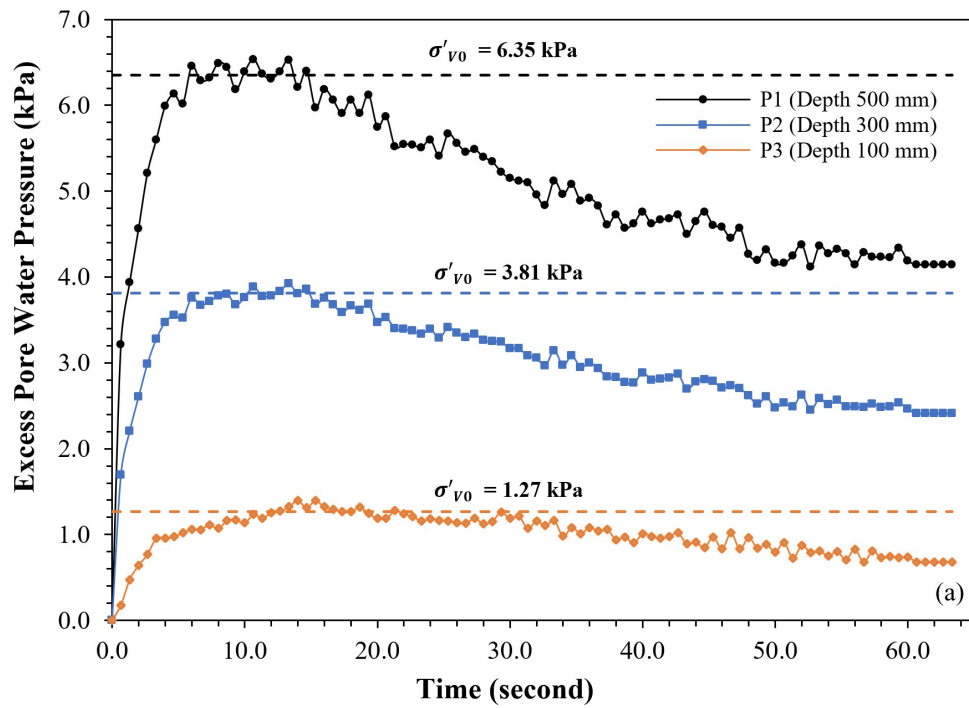
3. Results

3.1. Time History of Excess Pore Water Pressure

To evaluate the effect of depth on the response of saturated soil during dynamic loading, the evolution of excess pore water pressure (Δu) was analyzed at several depths with different initial effective overburden stresses (σ'_{v0}). Figure 8 shows the evolution of Δu against time at

three measurement depths (500 mm, 300 mm, and 100 mm) during dynamic loading.

Figure 8 shows the time histories of Δu measured at depths of 100 mm, 300 mm, and 500 mm under PGA of 0.3 g, 0.4 g, and 0.5 g. In all cases, Δu increases rapidly at the onset of shaking, reaches a peak, and subsequently dissipates, reflecting the typical undrained response of saturated sandy soil under cyclic loading.



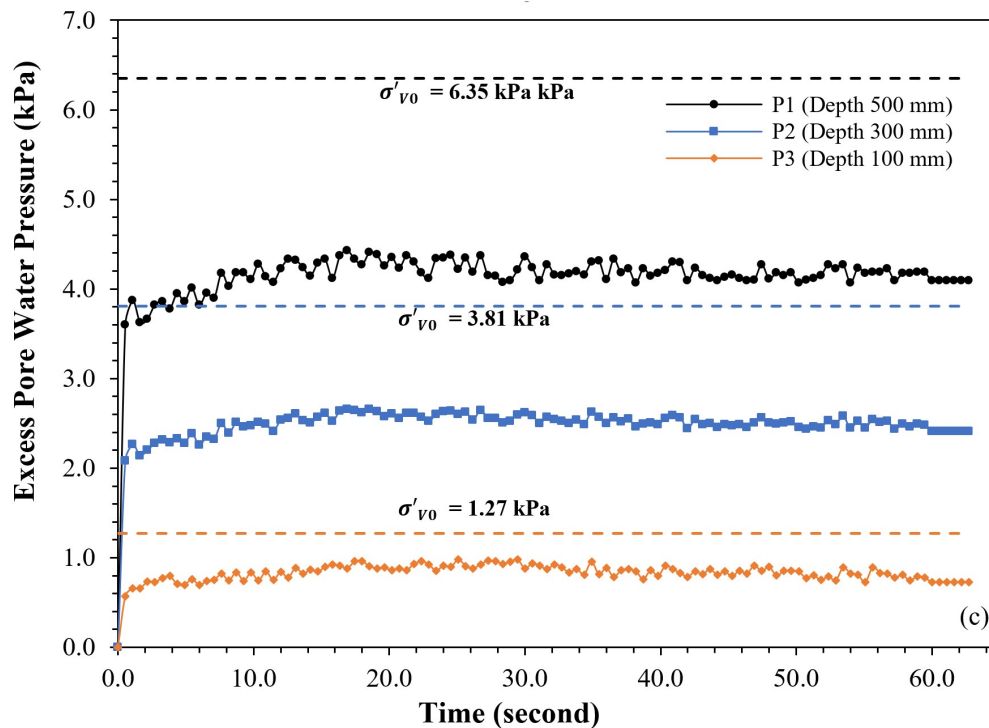


Figure 8. Time History of excess pore water pressure (Δu), a) PGA 0.3 g, b) PGA 0.4 g, c) PGA 0.5 g

At PGA = 0.3 g, significant pore pressure accumulation is observed at all depths, with the deepest layer exhibiting the largest absolute Δu values and the longest dissipation time. This indicates that moderate seismic loading is particularly effective in promoting pore pressure buildup under higher confinement and limited drainage conditions. Although the shallow layer shows higher pore water pressure ratio (ru) values due to lower initial effective overburden stress (σ'_{v0}), the deeper layer experiences more persistent excess pore water pressure accumulation.

Increasing the PGA to 0.4 g and 0.5 g accelerates the rate of pore pressure buildup but does not produce proportional increases in peak Δu . In several cases, lower peak values and shorter dissipation times are observed compared to those at PGA = 0.3 g, indicating a nonlinear relationship between PGA and pore water pressure response. This behavior is attributed to partial soil densification and enhanced drainage induced by stronger cyclic loading.

Overall, the results demonstrate that pore water pressure response in saturated sandy soil is strongly depth-dependent and nonlinear with respect to seismic loading intensity, with moderate PGA levels being more critical for pore pressure accumulation than higher acceleration levels.

3.2. Pore Water Pressure Ratio vs. PGA

To evaluate the effect of dynamic loading intensity on liquefaction potential, the relationship between the maximum pore water pressure ratio (ru_{max}) and PGA was analyzed at various depths under different initial effective

overburden stress conditions, as shown in Figure 9.

Figure 9 shows the relationship between the maximum pore water pressure ratio (ru_{max}) and PGA at three different measurement depths: 100 mm, 300 mm, and 500 mm. Generally, ru_{max} increases with higher PGA values at all depths, confirming that the intensity of dynamic loading primarily influences the formation of pore water pressure.

When the PGA reaches 0.3 g, the ru_{max} values at all depths approach or even reach one, particularly at shallower depths. This indicates a nearly complete loss of effective stress and the onset of liquefaction conditions, suggesting that a PGA of 0.3 g is a critical threshold for the tested soil.

As the PGA increases to 0.4 g and 0.5 g, the ru_{max} values decrease, dropping below one at all depths. This behavior indicates that with larger amplitude loads, dissipation and partial reconsolidation mechanisms become more prominent, thereby limiting the accumulation of maximum pore water pressure.

3.3. Excess Pore Water Pressure Ratio vs. Time

The relationship between Δu and time illustrates the dynamics of the response of saturated soil during seismic loading. Figure 10 shows the excess pore water pressure (Δu) values over time. Based on these values, the time parameter is divided into three phases: the excess pore water pressure rise phase (t_1), the excess pore water pressure peak time (t_2), and the excess pore water pressure dissipation phase (t_3). The values of each component are analyzed and presented in Table 4 and Figure 10.

Figure 10 shows that the phase of the increase in excess

pore water pressure (t_1) occurs earlier in the inner layer (P1, at a depth of 500 mm) than in the upper layer (P3, at a depth of 10 mm), with t_1 values ranging from 10 to 13.30 seconds. The increase in the t_1 value at a higher PGA (0.5 g) indicates that pore water pressure formation responds more quickly as vibration energy increases.

The peak phase (t_2) indicates the time at which the maximum value of excess pore water pressure is reached. In general, t_2 occurs between 2.68 and 3.30 seconds, with an increasing trend towards higher PGA values. For instance, at piezometer P1, the peak time decreased from 3.3 seconds (0.3 g) to 2.75 seconds (0.5 g). This suggests

that the soil becomes oversaturated more quickly under stronger earthquake loads, indicating an acceleration in the formation of liquefaction conditions.

The dissipation phase (t_3) is the period during which pore water pressure begins to decrease due to drainage or redistribution of pore water. The value of t_3 ranges from 40 to 47 seconds and generally decreases as PGA increases. This indicates that, although pore water pressure builds up more quickly under large earthquake loads, the stabilization process also occurs more quickly. This variation is possibly due to an increase in fractures or water flow paths within the soil mass.

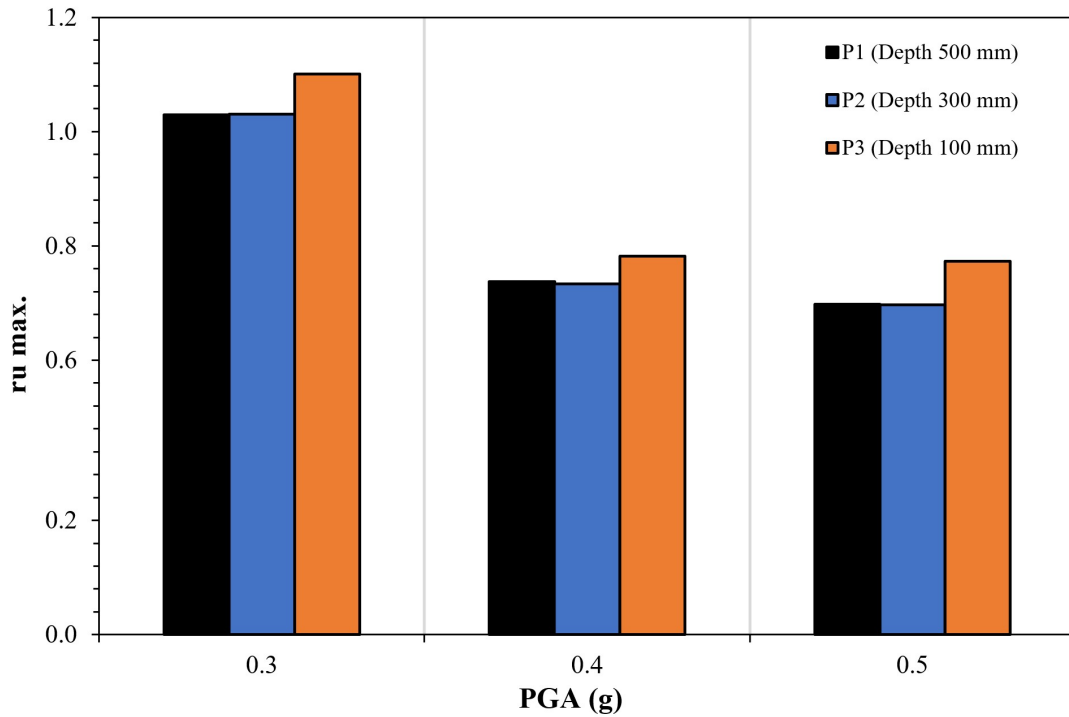
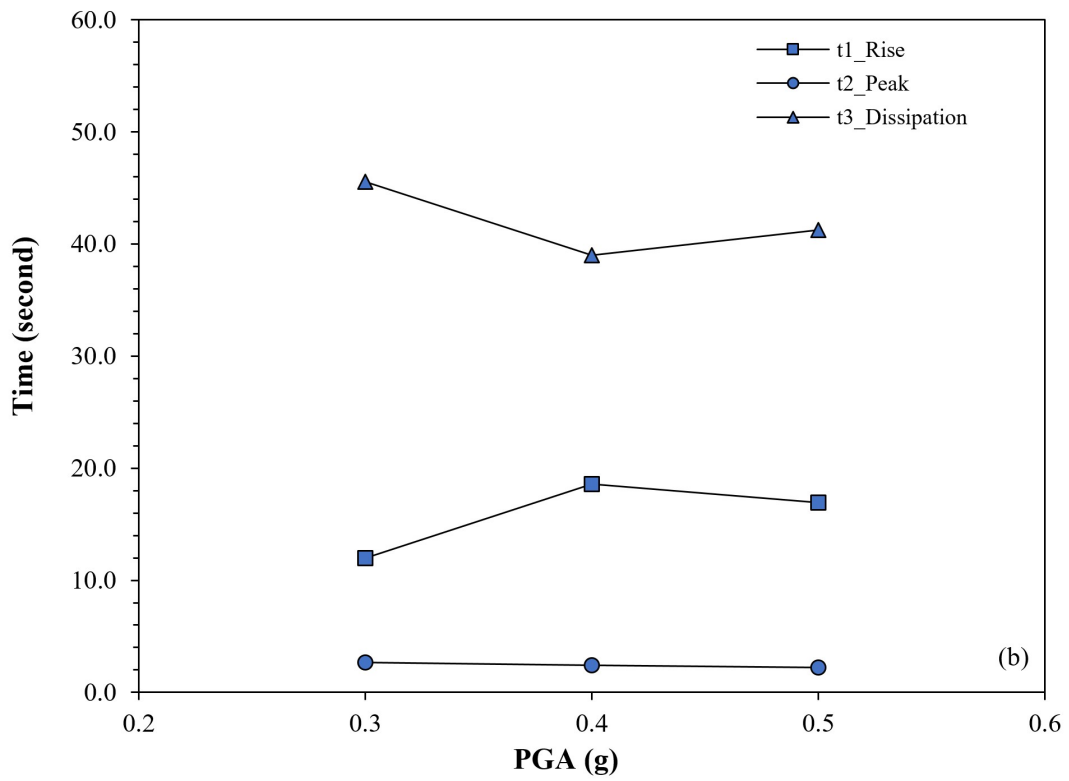
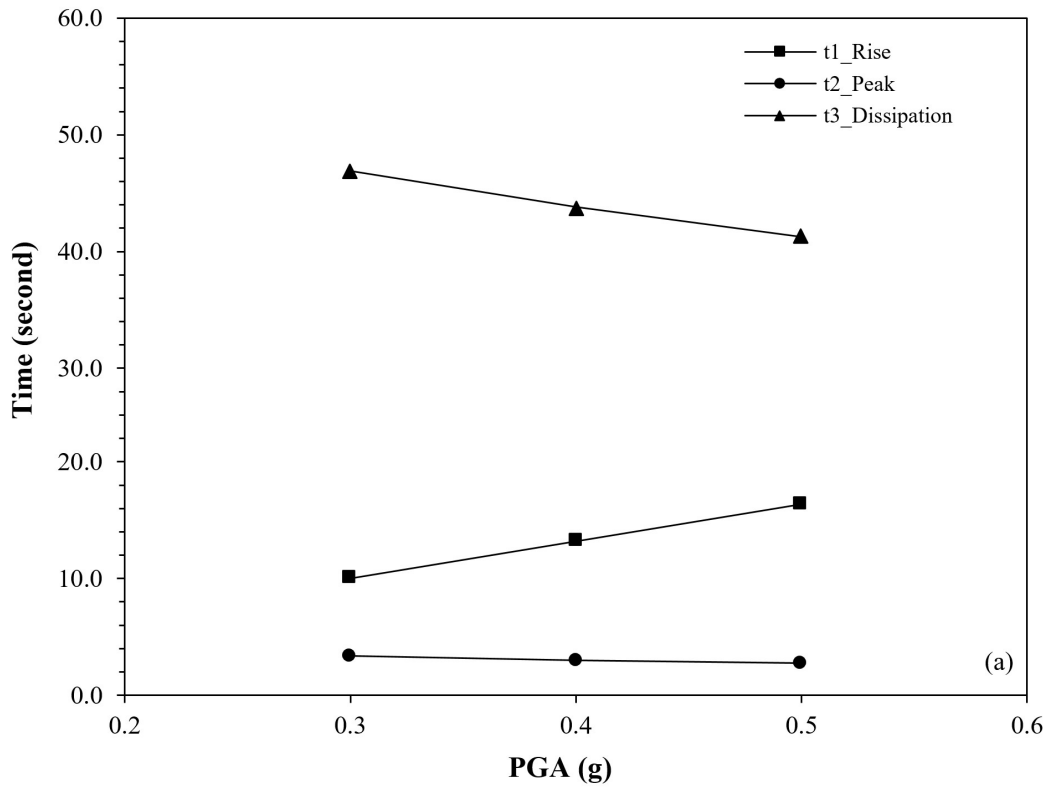


Figure 9. Summary of the maximum pore water pressure ratio (ru)

Table 4. Summary of Δu response times (t_1 : rise, t_2 : peak, t_3 : dissipation) at different depths for varying PGA

Description	Piezometer	PGA (g)		
		0,3	0,4	0,5
Phase of increase Δu (t_1) (second)	P1 (Depth 500 mm)	10.00	13.20	16.36
	P2 (Depth 300 mm)	12.00	18.60	16.91
	P3 (Depth 100 mm)	13.30	16.20	15.27
Peak phase of Δu (t_2) (second)	P1 (Depth 500 mm)	3.30	3.00	2.75
	P2 (Depth 300 mm)	2.68	2.40	2.20
	P3 (Depth 100 mm)	2.68	3.00	3.30
Phase of dissipation Δu (t_3) (second)	P1 (Depth 500 mm)	46.90	43.80	41.25
	P2 (Depth 300 mm)	45.56	39.00	41.25
	P3 (Depth 100 mm)	44.22	40.80	41.80



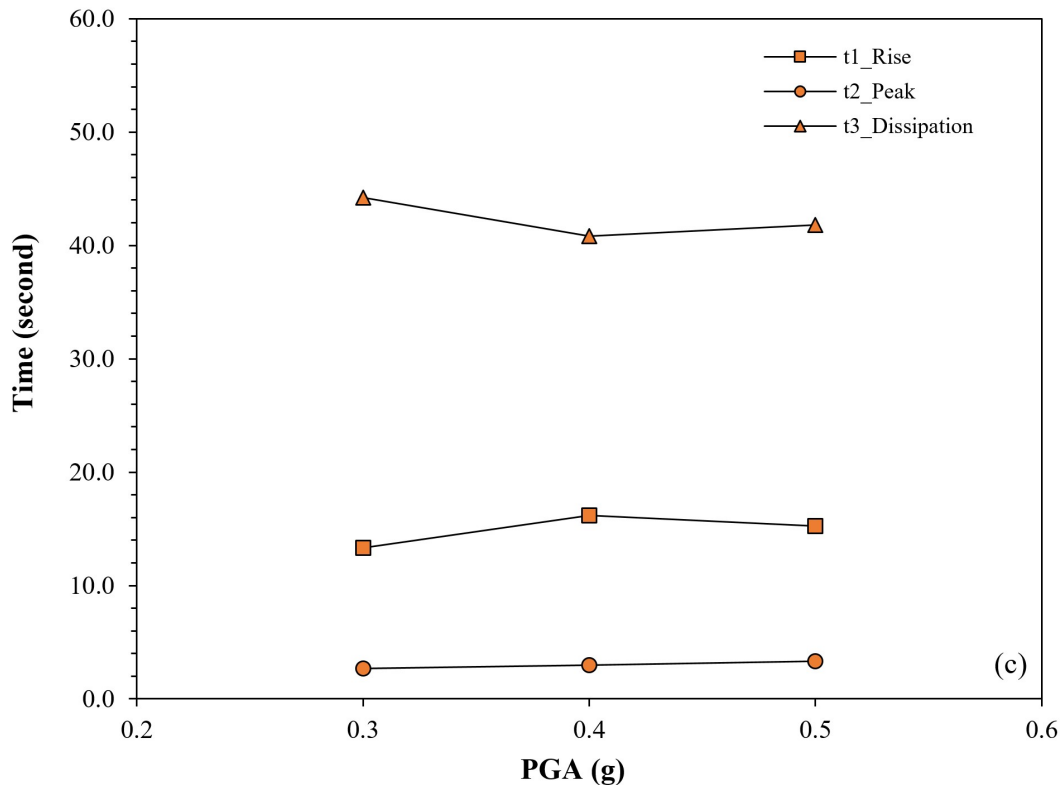


Figure 10. Phase of Δu increase (t_1), phase of peak excess pore water pressure (t_2), and phase of excess pore water pressure dissipation (t_3), (a) P1 (depth 500 mm), (b) P2 (depth 300 mm), and (c) P3 (depth 100 mm)

4. Discussion

The results of this study confirm that excess pore water pressure plays a dominant role in controlling liquefaction behavior under seismic loading. The observed increase in Δu and r_u with peak PGA, particularly at greater depths, is consistent with classical liquefaction mechanisms described by Seed and Idriss [5] and Ishihara [6], in which cyclic loading under undrained conditions leads to progressive loss of effective stress.

At moderate acceleration levels (PGA = 0.3 g), r_u values approaching unity were recorded in the lower layer, indicating conditions close to initial liquefaction. This depth-dependent response agrees with previous experimental and field studies that emphasize the influence of confinement stress and restricted drainage on pore pressure accumulation [5–7]. However, at higher acceleration levels (PGA \geq 0.4 g), the maximum Δu and r_u values exhibit a nonlinear response with respect to PGA. Similar nonlinear trends have been reported in shaking table studies by Ha et al. [8] and Wang et al. [10], [12], where strong cyclic loading promoted partial soil densification and enhanced permeability, resulting in accelerated pore pressure dissipation.

The temporal evolution of pore water pressure, characterized by distinct rise, peak, and dissipation phases, is consistent with observations reported in previous laboratory studies [10], [11]. From an engineering

perspective, these findings indicate that liquefaction potential cannot be assessed solely based on earthquake acceleration intensity, but must also consider soil density, depth, and drainage conditions. Despite limitations associated with small-scale testing and simplified loading conditions [8], [9], the comparative framework adopted in this study provides useful insights into the nonlinear and depth-dependent nature of pore water pressure response under seismic loading.

5. Conclusions

Shaking table tests conducted in this study demonstrate that pore water pressure development in saturated sandy soil exhibits a nonlinear response to peak ground acceleration. The experimental results show that Δu and r_u increase with seismic loading up to a critical level, with the highest values consistently occurring at PGA = 0.3 g, rather than at higher acceleration levels.

At this moderate PGA, r_u values approached unity, particularly in the deeper soil layer, indicating conditions close to the onset of liquefaction due to higher confinement and limited drainage. Further increases in PGA to 0.4 g and 0.5 g did not result in proportional increases in Δu or r_u , suggesting that stronger cyclic loading induced partial soil densification and enhanced pore water pressure dissipation, thereby limiting further pressure accumulation.

The pore water pressure response was characterized by three distinct temporal phases—buildup, peak, and dissipation—with higher PGA levels accelerating both pore pressure generation and recovery processes. These results indicate that liquefaction potential cannot be assessed solely based on earthquake acceleration intensity. Instead, soil depth, density, and drainage conditions play a critical role in governing pore water pressure evolution and effective stress degradation.

Despite the inherent limitations of laboratory-scale shaking table testing, this study provides experimental evidence that clarifies the depth-dependent and nonlinear mechanisms of pore water pressure response in saturated sandy soils. The findings contribute to a more robust understanding of liquefaction behavior and offer valuable implications for seismic hazard evaluation and ground improvement design in liquefaction-prone regions.

Acknowledgements

The authors gratefully acknowledge the support and financing of the Indonesian Education Scholarship, Center for Higher Education Funding and Assessment, and the Indonesian Endowment Fund for Education.

REFERENCES

- [1] F. Ishak Aksa, "INVESTIGATING THE ROLE OF GEOGRAPHY EDUCATION IN ENHANCING EARTHQUAKE PREPAREDNESS: EVIDENCE FROM ACEH, INDONESIA," *International Journal of GEOMATE*, vol. 19, no. 76, pp. 9–16, Dec. 2020, doi: 10.21660/2020.76.90006.
- [2] R. Rusnardi and J. Kiyono, "Estimation of Earthquake Ground Motion in Padang, Indonesia," *International Journal of GEOMATE*, vol. 1, no. 1, pp. 71–77, Oct. 2011.
- [3] H. Hazarika *et al.*, "Large distance flow-slide at Jono-Oge due to the 2018 Sulawesi Earthquake, Indonesia," *Soils and Foundations*, vol. 61, no. 1, pp. 239–255, Feb. 2021, doi: 10.1016/j.sandf.2020.10.007.
- [4] A. Arsyad, E. Syamsuddin, M. Azmi, M. Asyhari, and R. Wiryadiputra Suryadi, "A site-specific earthquake ground response analysis and relations to collapsing buildings in the 2021 Mw. 6.2 Mamuju-Majene Earthquake Sulawesi Indonesia," *Japanese Geotechnical Society Special Publication*, vol. 10, no. 26, p. v10.OS-15-03, 2024, doi: 10.3208/jgssp.v10.OS-15-03.
- [5] H. B. Seed and I. M. Idriss, "Simplified Procedure for Evaluating Soil Liquefaction Potential," *Journal of the Soil Mechanics and Foundations Division*, vol. 97, no. 9, pp. 1249–1273, Sep. 1971, doi: 10.1061/JSFEAQ.0001662.
- [6] K. Ishihara, "Liquefaction and flow failure during earthquakes," *Géotechnique*, vol. 43, no. 3, pp. 351–451, Sep. 1993, doi: 10.1680/geot.1993.43.3.351.
- [7] S. L. Kramer, *Geotechnical Earthquake Engineering*. New Jersey: Prentice Hall, 1996.
- [8] I. S. Ha, S. M. Olson, M. W. Seo, and M. M. Kim, "Evaluation of reliquefaction resistance using shaking table tests," *Soil Dynamics and Earthquake Engineering*, vol. 31, no. 4, pp. 682–691, Apr. 2011, doi: 10.1016/j.soildyn.2010.12.008.
- [9] I. Towhata, *Earthquake Geotechnical Engineering*. 2008.
- [10] B. Wang, K. Zen, G. Q. Chen, Y. B. Zhang, and K. Kasama, "Excess pore pressure dissipation and solidification after liquefaction of saturated sand deposits," *Soil Dynamics and Earthquake Engineering*, vol. 49, pp. 157–164, Jun. 2013, doi: 10.1016/j.soildyn.2013.02.018.
- [11] I. S. Ha, Y. H. Park, and Kim Myoung Mo, "Dissipation Pattern of Excess Pore Pressure After Liquefaction in Saturated Sand Deposits," *Transp Res Rec*, vol. 1821, no. 1, pp. 59–67, 2003, doi: 10.3141/1821-07.
- [12] B. Wang, K. Zen, G. Q. Chen, and K. Kasama, "Effects of excess pore pressure dissipation on liquefaction-induced ground deformation in 1-g shaking table test," *Geomechanics and Engineering*, vol. 4, no. 2, pp. 91–103, 2012, doi: 10.12989/gae.2012.4.2.091.
- [13] L. Z. Mase, "Experimental Liquefaction Study of Southern Yogyakarta Using Shaking Table Seismic Hazard Assessment of Bengkulu City View project dynamis View project Experimental Liquefaction Study of Southern Yogyakarta Using Shaking Table," *JURNAL TEKNIK SIPIL : Jurnal Teoritis dan Terapan Bidang Rekayasa Sipil*, vol. 24, no. 1, pp. 11–18, Apr. 2017, doi: 10.5614/jts.2017.24.1.2.
- [14] R. M. Varghese and G. M. Latha, "Shaking Table Studies on the Conditions of Sand Liquefaction," in *Geo-Congress*, American Society of Civil Engineers (ASCE), Feb. 2014, pp. 1244–1253. doi: 10.1061/9780784413272.121.
- [15] ASTM D4254 - 16, "Test Methods for Minimum Index Density and Unit Weight of Soils and Calculation of Relative Density," Mar. 01, 2016, *ASTM International*, West Conshohocken, PA. doi: 10.1520/D4254-16.
- [16] ASTM 4253 - 16, "Standard Test Methods for Maximum Index Density and Unit Weight of Soils Using a Vibratory Table," Mar. 01, 2016, *ASTM International*, West Conshohocken, PA. doi: 10.1520/D4253-16E01.
- [17] A. Ghorbani, H. Hasanzadehshooili, M. A. Somti Foumani, J. Medzvieckas, and R. Kliukas, "Liquefaction Potential of Saturated Sand Reinforced by Cement-Grouted Micropiles: An Evolutionary Approach Based on Shaking Table Tests," *Materials*, vol. 16, no. 6, Mar. 2023, doi: 10.3390/ma16062194.
- [18] D. Lombardi and S. Bhattacharya, "Shaking table tests on rigid soil container with absorbing boundaries," *15 th World Conference Earthquake Engineering*, 2012.
- [19] D. Lombardi, S. Bhattacharya, F. Scarpa, and M. Bianchi, "Dynamic response of a geotechnical rigid model container with absorbing boundaries," *Soil Dynamics and Earthquake Engineering*, vol. 69, pp. 46–56, Feb. 2015, doi: 10.1016/j.soildyn.2014.09.008.